

## Article

# The Formation of Small Amounts of Cyclopropane during Pulsed Pyrolysis of C<sub>4</sub>–C<sub>5</sub> Acyclic Alkanes in the Adiabatic Compression Reactor

Igor V. Bilera 

A.V. Topchiev Institute of Petrochemical Synthesis of the Russian Academy of Sciences (TIPS RAS), Leninsky Ave. 29, Moscow 119991, Russia; bilera@ips.ac.ru

**Abstract:** During high-temperature pulse pyrolysis of acyclic butanes and pentanes under adiabatic compression conditions, cyclopropane, a stressed cyclic hydrocarbon, was found among the reaction products in small quantities for the first time. The analysis of the reaction products was performed by gas chromatography using three capillary columns of different polarity, selectivity and sufficient efficiency. The identification of reaction products, including cyclopropane, was performed using retention times of individual substances and model mixtures, as well as comparing chromatograms with reference chromatograms from the literature and the ScanView Application Database. It was shown that the chromatographic peak attributed to cyclopropane could not be a ghost peak. Additional confirmation of this conclusion was obtained in a series of experiments on the pyrolysis of *n*-butane at a reduced initial temperature of the adiabatic compression reactor (from 120 °C to 50 °C) and a modified mode of GC analysis. Cyclopropane yields as a function of maximum temperature have a bell-shaped asymmetric dependence. The maximum value of the yield of cyclopropane increases with the transition from normal alkanes to isoalkanes, and from pentanes to butanes; for *n*-pentane, 0.009 wt. %, and for isobutene, ≈0.017 wt. %. During the pulse pyrolysis of isobutane, *n*-butane, isopentane and *n*-pentane, cyclopropane is not a primary product. Further theoretical and experimental studies are needed to establish the mechanism of cyclopropane formation during pyrolysis of C<sub>4</sub>–C<sub>5</sub> acyclic alkanes.

**Keywords:** pyrolysis; adiabatic compression; gas chromatography; butane; pentane; cyclopropane



**Citation:** Bilera, I.V. The Formation of Small Amounts of Cyclopropane during Pulsed Pyrolysis of C<sub>4</sub>–C<sub>5</sub> Acyclic Alkanes in the Adiabatic Compression Reactor. *Reactions* **2023**, *4*, 381–397. <https://doi.org/10.3390/reactions4030023>

Received: 25 May 2023  
Revised: 25 June 2023  
Accepted: 14 July 2023  
Published: 19 July 2023



**Copyright:** © 2023 by the author. Licensee MDPI, Basel, Switzerland. This article is an open access article distributed under the terms and conditions of the Creative Commons Attribution (CC BY) license (<https://creativecommons.org/licenses/by/4.0/>).

## 1. Introduction

The adiabatic compression (AC) of gas mixtures with a free piston is a homogeneous kinetics method applicable to the study of gas-phase reactions [1–8]. In this method, the gas mixture is rapidly heated during compression and cooled equally rapidly during expansion as the piston moves. During adiabatic compression, the maximum values of temperature ( $T_{\max}$ ) and pressure ( $P_{\max}$ ) can reach several thousand degrees and hundreds of atmospheres, respectively; the characteristic time of the method is several milliseconds [1,9–11]. One advantage of this method is the rapid heating and cooling of the reaction mixture, resulting in the ability to study fast reactions and reducing the role of secondary processes. Adiabatic compression is a convenient and reliable method for determining the detailed compositions of gas-phase reaction products of hydrocarbons, halogenated hydrocarbons and other substances in the medium and high temperature ranges [5–8,10–12]. Recently, there has been renewed interest in conducting reactions in piston reactors in which the gas mixture is heated and cooled in a periodic mode during compression and expansion. Such reactors are supposed to be used for the conversion of methane and other hydrocarbon raw materials into olefins and hydrogen [13,14], synthesizing gas [15], obtaining nanopowders [16], and other applications [17,18]. In piston reactors, compression occurs quickly, but still it cannot be considered adiabatic [11].

Using the AC method, the pulse pyrolysis of C<sub>4</sub>–C<sub>5</sub> alkanes of normal and isometric structures (isobutane [19], *n*-butane [20], *n*-pentane [21] and isopentane [22]) was studied in the temperature range 950–1520 K and in a wide range of conversion degrees (0.2–95%). Chemical analysis of the compositions of the initial mixtures (1–2% alkane + argon) and the reaction products was carried out by gas chromatography. A capillary column with molecular sieves and a thermal conductivity detector with a small internal volume (microTCD) were used to determine H<sub>2</sub>, and the carrier gas was argon. A detailed analysis of the hydrocarbon mixture was carried out using an Al<sub>2</sub>O<sub>3</sub>/KCl PLOT capillary column and a flame ionization detector (FID), with helium as the carrier gas. For example, for each of the above alkanes, the following C<sub>4</sub> hydrocarbons were detected among the product mixtures studied: *n*-butane, isobutane, butene-1, *trans*- and *cis*-butenes-2, isobutene, butadiene-1,3, vinyl acetylene, diacetylene, butene-1 and butene-2 (see Figures S1 and S2). However, several unidentified low-height peaks remained in the FID chromatograms of the pyrolysis product mixtures. Among them is the peak located before the propylene peak (see Figures S3–S6). The height of this peak varies smoothly from experiment to experiment depending on the temperature reached during compression. In the analyses of the initial C<sub>4</sub>–C<sub>5</sub> alkane mixtures, this peak was absent in the FID chromatograms (red chromatograms in Figures S3–S6). A comparison of the obtained chromatograms with reference chromatograms from ScanView Application Database [23] showed the only candidate for identification of this peak—cyclopropane *cyclo*-C<sub>3</sub>H<sub>6</sub>.

The pyrolysis of alkanes of normal and isomeric structure, including butanes and pentanes, is well studied [24–27]. The mechanisms of gas-phase pyrolysis of lower alkanes have common features. In general, the composition of pyrolysis products of lower alkanes is almost the same, although there are some differences in the reaction products of normal and isoalkanes [26,28]. The main pyrolysis products of butanes and pentanes are: hydrogen, methane, ethylene and propylene. Among the minor reaction products are: olefins (butenes, pentenes), dienes (allene, butadiene and others), acetylenes (acetylene, methylacetylene and others), alkanes (ethane, propane, *n*-butane), benzene, and toluene. Cyclopropane was not detected among the pyrolysis products of acyclic butanes and pentanes.

Cyclopropane is the cyclic alkane with the least carbon atoms. Functionally substituted cyclopropanes exist in nature [29,30], but unsubstituted cyclopropane does not occur in natural objects. Due to high cycle tensions, cyclopropane and its derivatives can be obtained only using special methods [31–34]. In particular, cyclopropane is formed during the dehalogenation of 1,3-dihalopropane [35], during addition to ethylene of methylene CH<sub>2</sub> generated by photolytic or thermal decomposition of diazomethane [36] or ketene [37], and during photochemical or thermal decomposition of 1-pyrazoline with N<sub>2</sub> extrusion [38] and cyclobutanone with CO extrusion [39,40].

Few cases are known wherein cyclopropane is formed directly from hydrocarbons in a thermal reaction. It is established that cyclopropane is formed as a minor primary product in the pyrolysis of cyclopentane in a shock tube, in the temperature range 1050–1220 K [41], and in a VLPP reactor [42], but not in the pyrolysis of cyclohexane [43,44]. Small amounts of cyclopropane were found in the decay products of the 5-methyl-1-hexyl radicals and 1-pentyl radicals obtained by shock tube heating of 5-methylhexyl iodide [45] and 1-iodopentane [46], as well as the cyclopentyl radical obtained from cyclopentane by detaching the H atom [47], but not from the cyclopentyl radical, obtained as a result of the attachment of the H atom to the cyclopentene [48]. The theoretically possible formation of cyclopropane as a result of the reaction of ethylene and methylene generated during the decomposition of the precursor hydrocarbon molecule requires high energy input and, to our knowledge, has not been found experimentally. In particular, to obtain CH<sub>2</sub> via the thermal decomposition of ethane, it is necessary to heat up to the temperature 2100 K and more [49]; therefore, this variant of the formation of cyclopropane at pyrolysis of C<sub>4</sub>–C<sub>5</sub> alkanes [19–22] is excluded. As far as is known from the literature, in works where the detailed analysis of hydrocarbons by the GC method was undertaken, cyclopropane was not observed among the products of pyrolysis of *n*-pentane [27,28,50], isopentane [28]

and higher alkanes of normal and isomeric structures [27,28]. In the pyrolysis products of *n*-butane and isobutane yielded by synchrotron vacuum UV photoionization mass spectrometry (SVUV-PIMS) techniques, a large number of products were determined, but not cyclopropane [51,52]. Cyclopropane is also absent among the products of *n*-butane pyrolysis in a quasi-wall-free reactor using laser heating [53] and flow reactors [54].

So, according to the literature data, the formation of cyclopropane during the pyrolysis of hydrocarbons in the temperature range 1050–1220 K was found only with the decomposition of cyclopentane. Two paths were suggested for this reaction: the decomposition of the cyclopentane molecule to form 1,5-biradical followed by its decomposition into ethylene molecule and 1,3-biradical (trimethylene  $\cdot\text{CH}_2\text{CH}_2\text{CH}_2\cdot$ ), which closes into the cyclopropane molecule [41], or the immediate decomposition of the cyclopentane molecule into ethylene and cyclopropane molecules [55]. For the pyrolysis of  $\text{C}_4$ – $\text{C}_5$  alkanes of normal and isomeric structures, both these variants—release of 1,3-biradical  $\cdot\text{CH}_2\text{CH}_2\text{CH}_2\cdot$  or cyclopropane molecules—seem to be unlikely. The presence of cyclopropane in the pyrolysis products of acyclic alkanes  $\text{C}_4$ – $\text{C}_5$  can update the kinetic schemes of pyrolysis of lower hydrocarbons, so the establishment of the actual state of affairs is of great interest. Therefore, a study was undertaken to identify a minor product formed during the pulsed pyrolysis of  $\text{C}_4$ – $\text{C}_5$  alkanes and eluting on an  $\text{Al}_2\text{O}_3/\text{KCl}$  PLOT capillary column before the propylene peak. For the trustworthy identification of cyclopropane, chemical analysis by gas chromatography was performed using three capillary columns with different polarity and selectivity. The selected capillary columns had sufficient efficiency for the separation of lower hydrocarbons, which is important for reliable identification.

## 2. Materials and Methods

### 2.1. Adiabatic Compression of Gases with Free Flying Piston

The pulse pyrolysis of  $\text{C}_4$ – $\text{C}_5$  alkanes was studied by adiabatic gas compression with free flying piston. Gas compression is adiabatic if there is no heat exchange between the compressed gas and the reactor walls. For this, the compression must be so fast that the characteristic times of this process become shorter than the characteristic times of transport processes such as thermal conduction and diffusion. If the gas is compressed at speeds lower than the speed of sound, no shock waves occur. For an ideal gas with a constant heat capacity (perfect gas), such compression is isentropic and is described by the Poisson adiabatic equation [8,9,11]:

$$T = T_0 \varepsilon^{\gamma-1}, \quad P = P_0 \varepsilon^{\gamma} \quad (1)$$

where  $T$  (K) and  $P$  (atm) are the temperature and pressure of the compressible gas,  $T_0$  and  $P_0$  are the initial values of the temperature and pressure of the gas,  $\varepsilon = V_0/V$  geometric degree of compression,  $V_0$  and  $V$  are the initial and current values of gas volume,  $\gamma = C_p/C_v$  adiabatic coefficient, and  $C_p$  and  $C_v$  are the specific heat capacities at constant pressure and constant volume, respectively.

In the pneumatically actuated adiabatic free piston compression reactor, the piston moves freely under the influence of the pressure difference between the driver gas and the mixture under study. The mixture is compressed by the work of the driver gas, initially pressurized in the receiver and fed by the rapid opening of the valve into the space behind the piston. When the mixture under study is compressed, its volume decreases, and its pressure and temperature increase (heating occurs). The piston stops when the forces acting on the piston become equal. It then starts moving in the opposite direction, and the studied gas expands and cools down. In the following experiments, increases in the pressure of the driver gas in the receiver with the constant initial composition of the studied gas and invariable values of initial parameters ( $T_0$ ,  $P_0$ ,  $V_0$ ) will lead to increases in the value of the maximum degree of compression  $\varepsilon_{\text{max}}$ , and accordingly in the values of the maximum temperature  $T_{\text{max}}$  and pressure  $P_{\text{max}}$ . In the process of compression–expansion of the studied mixture, the temperature of the reactor walls does not change, which ensures that the reactor walls do not influence the reaction.

## 2.2. Experimental Setup

A schematic of the experimental adiabatic compression setup (ACS) is shown in Figure 1 (in various articles the adiabatic compression reactor is referred to as ballistic compressor [56], ballistic piston compressor [10], adiabatic compressor [57] or ballistic piston apparatus [1]). The main element of the ACS is the reactor, which is a thick-walled, horizontally placed cylinder made of high-strength steel. The inner channel of the cylinder is manufactured with high accuracy (deviation from cylindricity at the length of the reactor is less than 0.01 mm). The cylinder is closed at both ends with removable flanges.

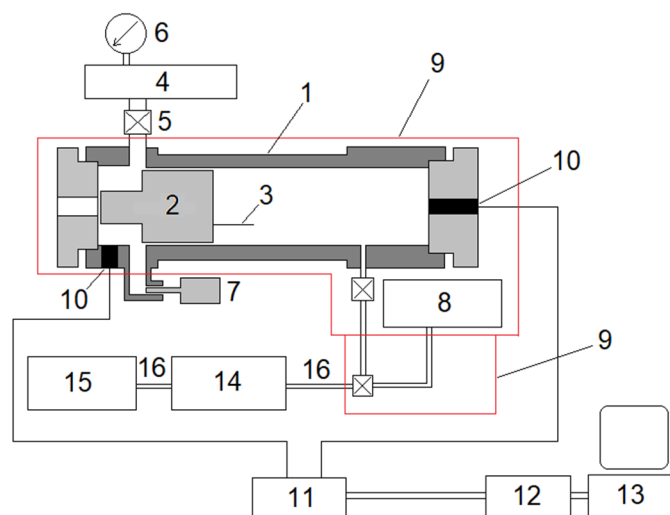


**Figure 1.** Schematic diagram of the experimental setup. 1—cylinder, 2—piston, 3—a compression degree indicator, 4—driver gas receiver, 5—valve, 6—manometer, 7—back-pressure valve, 8—feedstock container, 9—air thermostat, 10—pressure transducer, 11—charge amplifier, 12—analogue-to-digital converter, 13—personal computer, 14 and 15—gas chromatographs, 16—heated capillary.

The piston is inside the cylinder. The piston is fitted to the cylinder with a clearance of  $\sim 0.01$  mm, thus achieving a good seal without rings and lubrication. In this paper, a titanium alloy piston weighing 464 g was used. At the end of the piston, there was an orifice for fastening a compression degree indicator—a soft aluminum wire with a flattened end, which deforms on impact with a blind cylinder bottom. By measuring the length of this wire after the experiment, the minimum distance between the piston and the bottom of the cylinder in each experiment was determined, by which the maximum geometric compression ratio was calculated  $\varepsilon_{\max}: \varepsilon_{\max} = V_0/V_{\min} = L/x_{\min}$ , where  $L$  and  $x_{\min}$  are the length of the part of the cylinder filled with the test gas before the experiment and at the time of maximum compression.

In order to ensure a one-time compression–expansion process, an inertia valve (back-pressure valve) is located in the space behind the piston, which at the right moment opens the driver gas to the atmosphere.

The reactor and the feedstock container with the gas mixture to be tested are placed in an air thermostat. The rest of the gas line system with shut-off valves is placed in a second thermostat directly adjacent to the main thermostat. The mixtures of substances from the reactor or the feed container are fed for analysis to the chromatographs via a heated metal capillary.

The pressure in the reactor working volume  $P_1(t)$  and in the piston space  $P_2(t)$  was measured by means of piezoquartz pressure transducers model 7031 (0–250 bar) manufactured by Kistler (Winterthur, Switzerland). The signal of the pressure sensors was transmitted to a personal computer by means of an analog-to-digital converter (ADC) L-1250 by L-card (Moscow, Russia).

Main parameters of the ACS: internal diameter of the cylinder 42.15 mm, working length of the cylinder  $L = 432$  mm, volume of the investigated gas 0.60 L, volume of the

driver gas receiver 0.47 L. Nitrogen of 99.996% purity was used as the driver gas. The pressure in the driver gas reservoir  $P_{rev}$  was determined using a manometer.

In this study, in all experiments the initial pressure of the gas mixture in the reactor  $P_0 = 1$  atm. For the four series of experiments with isobutane, *n*-butane, isopentane and *n*-pentane, the initial temperature  $T_0 = 120$  °C (393 K). For *n*-butane, an additional series of experiments was performed with  $T_0 = 50$  °C (323 K) and modified sample entry and analysis conditions (see below for details).

### 2.3. Materials

The purity of the starting components according to GC data was as follows: isobutane 99.40 wt. % (main impurities: *trans*-C<sub>4</sub>H<sub>8</sub> 0.19, butene-1 0.14, *cis*-C<sub>4</sub>H<sub>8</sub> 0.13, *n*-butane 0.08 wt. %); *n*-butane 99.16 wt. % (main impurities: neopentane 0.30, isobutane 0.17, propane 0.13, propylene 0.13, butenes sum 0.05 wt. %); *n*-pentane 98.91 wt. % (main impurities: isopentane 0.89, *n*-hexane 0.10, 2-methylpentane 0.04 wt. %); isopentane 99.89 wt. % (main impurities: 2-methylbutene-2 0.06 wt. %).

Cyclopropane was synthesized according to the method in [35]. The purity of the sample according to <sup>1</sup>H-NMR analysis is 98%. <sup>1</sup>H-NMR analysis was performed on a Bruker AM300 (ZIOC RAS, Moscow, Russia). Two reference mixtures were made: 15 ppm cyclopropane in argon and 15 ppm cyclopropane and 15 ppm propylene in argon. A reference mixture Scott (Supelco, Bellefonte, PA, USA) was also used for the identification of substances: 15 ppm CH<sub>4</sub>, C<sub>2</sub>H<sub>6</sub>, C<sub>2</sub>H<sub>4</sub>, C<sub>2</sub>H<sub>2</sub>, C<sub>3</sub>H<sub>8</sub>, C<sub>3</sub>H<sub>6</sub>, C<sub>3</sub>H<sub>4</sub>, *n*-C<sub>4</sub>H<sub>10</sub> in nitrogen (15 ppm C<sub>n</sub>H<sub>m</sub> in N<sub>2</sub>).

Initial mixtures containing isobutane and *n*-butane and reference mixtures containing cyclopropane were composed by pressure. To prepare mixtures containing *n*-pentane and isopentane, the calculated amount of liquid alkane was injected using a syringe into the prepared feedstock container (through a vacuum-tight rubber) and then the required amount of argon (neon and argon, in the case of isopentane) was added. The compositions of the initial mixtures (% vol.): isobutane 2.0, argon 98.0; *n*-butane 2.0, argon 98.0; isopentane 0.86, neon 0.22, argon 98.9; *n*-pentane 1.0, argon 99.0.

The purity of the gases for GC analysis: He 99.995%, Ar 99.998%, H<sub>2</sub> 99.99%. Commercial filters for the preparation of carrier gases were used: oxygen and moisture for He, moisture for Ar. Air was supplied from pre-compressed gas cylinders. Parker Balston (Parker Hannifin Corporation, Lancaster, NY, USA) zero air generator and filters absorbing residual hydrocarbons and moisture were used for air purification.

### 2.4. GC Analysis

Chemical analysis of the starting mixtures and process products was carried out by gas chromatography. Typically Varian CP-3800 (Middelburg, The Netherlands) and Chrompack CP 9000 (Middelburg, The Netherlands) chromatographs were used. Each was equipped with a thermal conductivity detector (microTCD or TCD) and a flame ionization detector (FID). Each analytical channel had two sample introduction devices: an injector and downstream gas-sampling valve Valco WE or UWE-series (Valco Instruments Co. Inc., Houston, TX, USA).

The initial mixture was kept at overpressure in a feedstock container (metal cylinder) placed in the same thermostat as the reactor. After completion of the compression–expansion cycle, the reaction products were inside the reactor at atmospheric pressure. The feed of the sample from the feed tank and from the reactor for analysis in the chromatographs was carried out using a metal capillary heated to reactor temperature (120 °C), and the dosing of samples into the chromatographic columns was done using Valco gas sampling valves heated to 150 °C. The temperature of all injectors was 150 °C.

The separation of hydrocarbons was carried out on a capillary column CP-Al<sub>2</sub>O<sub>3</sub>/KCl PLOT 50 m × 0.53 mm × 10 μm (Varian, Middelburg, The Netherlands), with a detector of FID (T = 220 °C, carrier gas—helium). Detectable components: C<sub>1</sub>–C<sub>4</sub> hydrocarbons

(detailed), pentanes (*n*-, *iso*-, *neo*- and *cyclo*-), pentenes (6 acyclic and cyclopentene), isoprene, cyclopentadiene, benzene, toluene (see Figures S1 and S2).

A second FID ( $T = 220\text{ }^{\circ}\text{C}$ , carrier gas—helium) and a porous polymer column were used to determine the components of the critical pairs: allene and isobutane in isobutane pyrolysis and methylacetylene and isopentane in isopentane pyrolysis. There were two options: a CP-PoraBOND Q  $25\text{ m} \times 0.53\text{ mm} \times 10\text{ }\mu\text{m}$  capillary column (Varian, The Netherlands/USA) and a CP-PoraPLOT U  $25\text{ m} \times 0.53\text{ mm} \times 20\text{ }\mu\text{m}$  capillary column (Varian, The Netherlands/USA). The former is comparable in polarity with the well-known non-polar porous polymer Porapak Q, and the latter is comparable in polarity with the polar porous polymer Porapak N [58]. In the three capillary PLOT columns used in this work with FID detectors, the selectivity increased in the series: porous polymer Q type < porous polymer U type <  $\text{Al}_2\text{O}_3/\text{KCl}$  [59]. The efficiency of all three columns, especially the CP- $\text{Al}_2\text{O}_3/\text{KCl}$  PLOT column, was sufficient for the analysis of light hydrocarbon mixtures, which is important for the identification of unknown substances [60].

The analysis of permanent gases and the determination of hydrogen was carried out with a micro thermal conductivity detector (micro-TCD,  $T = 110\text{ }^{\circ}\text{C}$ ), and the carrier gas was argon, with separation on a Molsieve 5A PLOT  $25\text{ m} \times 0.53\text{ mm} \times 50\text{ }\mu\text{m}$  capillary column (Chrompack, Middelburg, The Netherlands). The second thermal conductivity detector (TCD) used helium as the carrier gas. This detector and the  $3\text{ m} \times 2\text{ mm}$  column filled with HayeSep Q 80/100 porous polymer (Hayes Separations, Bandera, TX, USA) were used to determine the composition of the initial mixture.

In an additional series of experiments, an Agilent 6890N (Agilent Technologies, Inc., Santa Clara, CA, USA) equipped with an FID detector ( $T = 220\text{ }^{\circ}\text{C}$ , carrier gas—helium) was used along with the two chromatographs mentioned above. The sample was fed into an Agilent 6890N (Agilent Technologies, Inc.) chromatograph equipped with a CIS4 cooled injection system using gas syringes. Separation was performed on one of the two porous polymer columns, and the carrier gas was helium.

Peak identifications were made for individual compounds and for standard mixtures. The identification of vinylacetylene, diacetylene and cyclopentadiene, as well as the confirmation of the identification of isoprene, benzene and toluene, were carried out by chromatography–mass spectrometry in the TIPS RAS chromatography laboratory.

### 3. Results and Discussion

#### 3.1. Pressure–Time History and Calculation of $T_{max}$

Examples of the experimental pressure dependence of the compressible gas  $P_1(t)$  at different values of the driver gas pressure are shown in Figure 2. The moment of maximum compression was chosen as  $t = 0$ , so negative time values correspond to gas compression and positive time values to expansion.

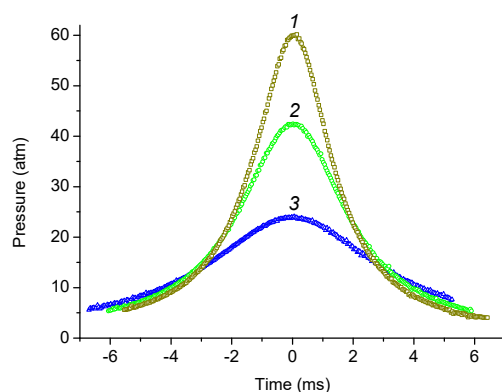


**Figure 2.** Comparison of pressure dependencies during adiabatic compression of a mixture of 2.0% vol. *n*-butane, 98% argon.  $T_0 = 393\text{ K}$  ( $120\text{ }^{\circ}\text{C}$ ). Pressures of driver gas: 1—12.0 atm; 2—10.0 atm; 3—7.0 atm. Skip 2 points on the pressure dependences.

For each experiment, the experimentally determined maximum pressure  $P_{\max}$  of compressible gas and compression ratio  $\varepsilon_{\max}$  were used to calculate the maximum temperature  $T_{\max}$  using the Clapeyron formula:

$$T_{\max} = \frac{P_{\max} \cdot V_{\max} \cdot T_0}{P_0 \cdot V_0} = \frac{P_{\max} \cdot T_0}{P_0 \cdot \varepsilon_{\max}} \quad (2)$$

### 3.2. Choosing of Temperature Programmes for GC Analysis

The choice of chromatographic columns for the separation of product mixtures was guided by the need to ensure the most complete separation of components, including small components, so that the small components are not masked by the main product peaks. For the chemical analysis of a complex mixture of light hydrocarbons, PLOT columns are the most suitable. The use of WCOT columns for this purpose involves cooling the column thermostat initially to negative temperatures. To determine cyclopropane in a complex mixture of light hydrocarbons, it is possible to use columns with methyl silicone phase, for example CP-Sil 5CB [61], but the pyrolysis products of  $C_4$ – $C_5$  alkanes have high propylene content as well as methyl acetylene and allene; therefore, a small cyclopropane peak, eluting the last of the  $C_3$  hydrocarbons, will be masked by peaks of these  $C_3$  hydrocarbons. Using PLOT columns with alumina and porous polymers, mixtures of  $C_1$ – $C_4$  and  $C_1$ – $C_3$  hydrocarbons, respectively, can be separated to the base line.

It is known that the elution order of light hydrocarbons of different classes on all PLOT columns with alumina remains unchanged in almost all cases, except for the analysis of alkynes and dienes when using an  $Al_2O_3/KCl$  column [62]. For this column, the elution order of the hydrocarbons can vary depending on the temperature program. In the literature, there are many examples of the separation of light hydrocarbon mixtures, including those with cyclopropane, on capillary columns with alumina deactivated with KCl [59,62–70]. In all these cases, the order of elution of  $C_3$  hydrocarbons was established: propane, cyclopropane, propylene, allene and methylacetylene. Six applications (reference chromatograms) obtained using CP- $Al_2O_3/KCl$  PLOT capillary columns of different length, inner diameter and thickness of the adsorbent layer are shown in Table 1. These reference chromatograms were obtained in isothermal mode and by programming the oven temperature, with initial temperature values from 40 to 100 °C. The reference chromatograms show peaks of five  $C_3$  hydrocarbons (propane, cyclopropane, propylene, allene, methylacetylene) along with other light hydrocarbons. In these reference chromatograms, the cyclopropane peak precedes the propylene peak. When the initial temperature is increased to 130 °C, the cyclopropane and propylene peaks elute together (Application A00273 + [67]). The reverse elution order, i.e., propylene first followed by cyclopropane, is not observed for the CP- $Al_2O_3/KCl$  PLOT capillary columns.

**Table 1.** Application numbers from the ScanView Application Database [23] used for comparison with chromatograms.

GC Column	Application No.
CP- $Al_2O_3/KCl$ PLOT	A00155, A00677, A01099, A01123, A01124, A01545
CP-PoraBOND Q	A01454
CP-PoraPLOT U	A01456, CA000C1128

The analysis of initial mixtures, mixtures of pyrolysis products and reference mixtures using a CP- $Al_2O_3/KCl$  PLOT capillary column was performed according to the following standard temperature oven program: 100 °C—12 min, temperature rise 8 °C/min to 188 °C. The total analysis time was 60 min or more if necessary. Cyclopropane and propylene peaks were eluted at the first temperature plateau at 100 °C. Thus, conditions were created for their separation as separate peaks. Examples of analyses of light hydrocarbon mixtures, including those involving cyclopropane, are shown in Figures 3, 4a and S3–S6.

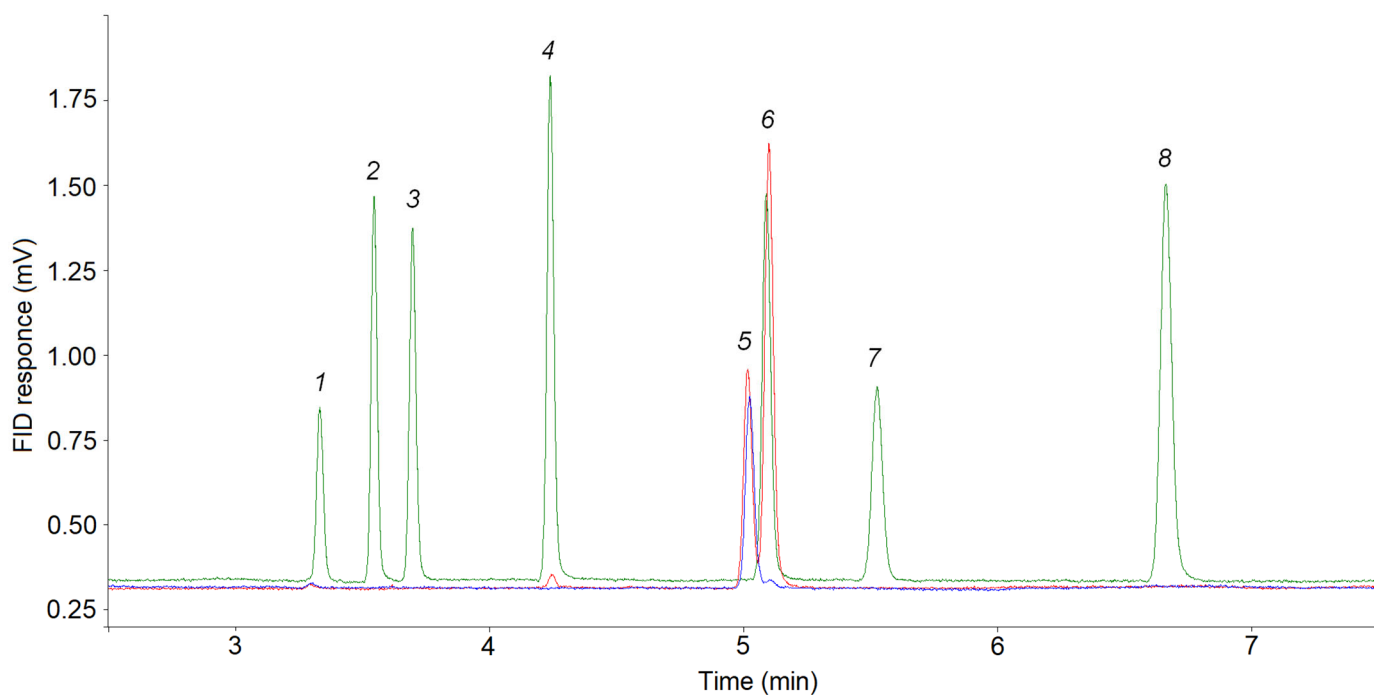


**Figure 3.** Separations of C<sub>1</sub>–C<sub>3</sub> hydrocarbons on the CP-Al<sub>2</sub>O<sub>3</sub>/KCl PLOT column. Blue line—reference mixture 15 ppm cyclopropane in Ar, red line—reference mixture 15 ppm cyclopropane + 15 ppm propylene in Ar, green line—reference mixture 15 ppm C<sub>n</sub>H<sub>m</sub> in N<sub>2</sub>. Peaks: 1 = methane; 2 = ethane; 3 = ethylene; 4 = propane; 5 = cyclopropane; 6 = propylene; 7 = acetylene; 8 = *n*-butane.

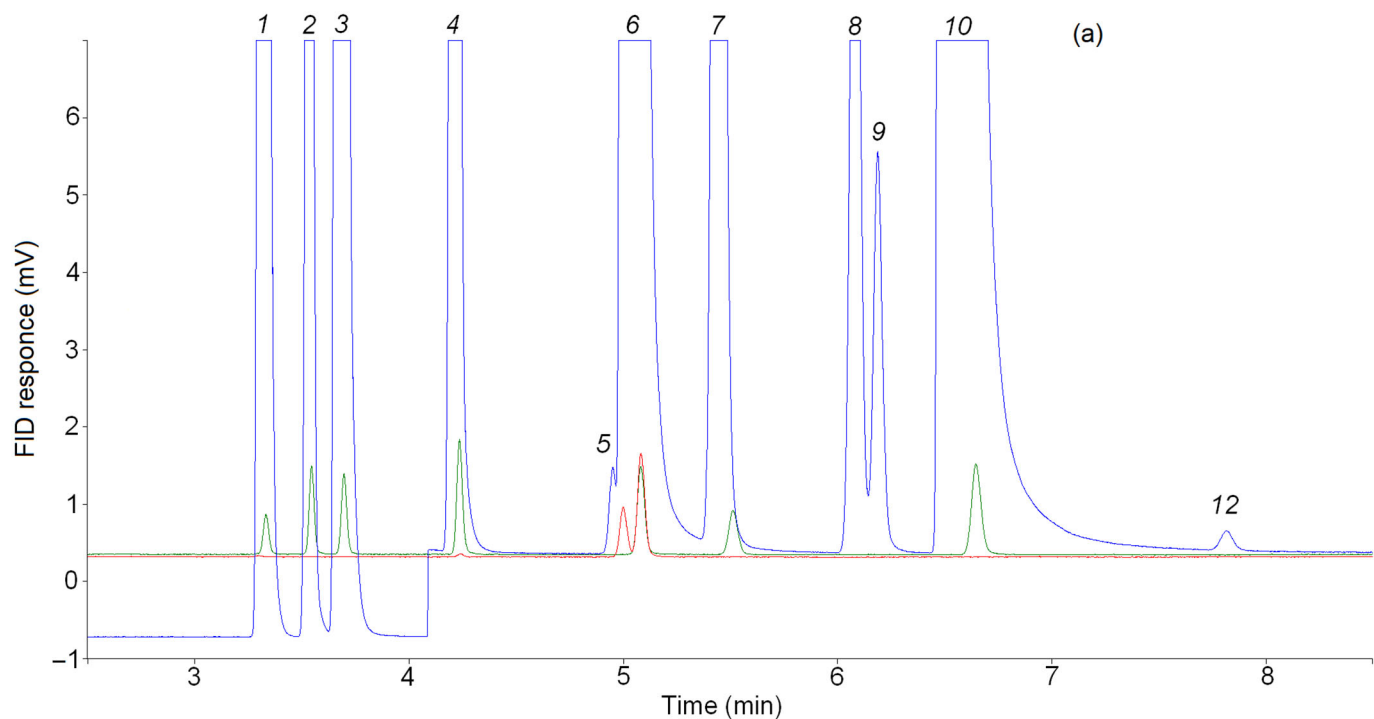


**Figure 4.** Cont.

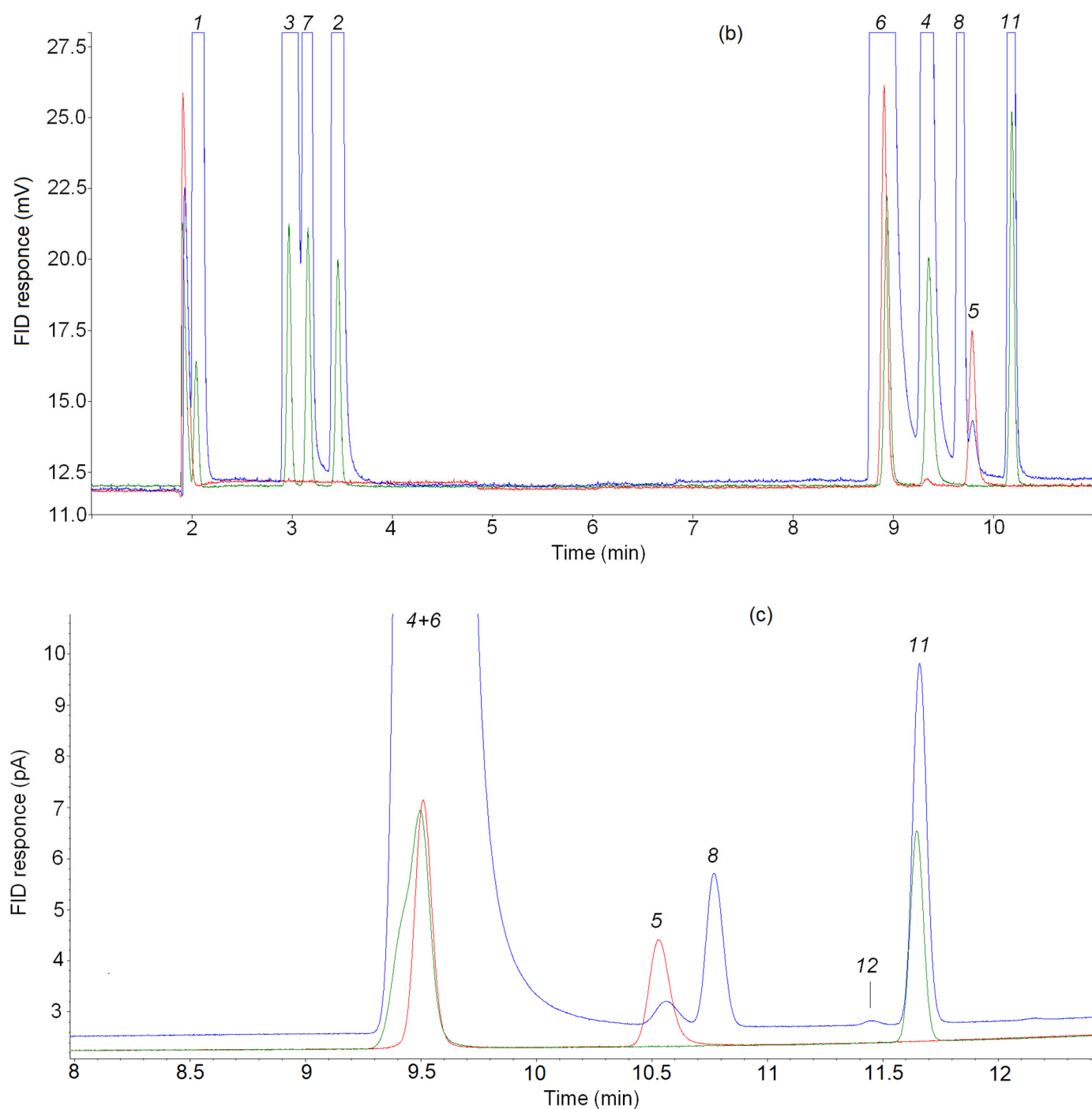


**Figure 4.** Separations of C<sub>3</sub> hydrocarbons on (a) the CP-Al<sub>2</sub>O<sub>3</sub>/KCl PLOT, (b) the CP-PoraBOND Q and (c) the CP-PoraPLOT U columns. Blue line—products of *n*-butane pyrolysis, red line—reference mixture *cyclo*-C<sub>3</sub>H<sub>6</sub>/15 ppm C<sub>3</sub>H<sub>6</sub> in Ar, green line—reference mixture 15 ppm C<sub>n</sub>H<sub>m</sub> in N<sub>2</sub>. Note that the larger peaks are off-scale to allow observation of the minor substances. Peaks: 1 = methane; 2 = ethane; 3 = ethylene; 4 = propane; 5 = cyclopropane; 6 = propylene; 7 = acetylene; 8 = allene; 9 = isobutane; 10 = *n*-butane, 11 = methylacetylene, 12 = unknown substance.

In an additional series of experiments on the pyrolysis of *n*-butane (2a), along with a decrease in reactor temperature to  $T_0 = 323$  K (50 °C), the temperature regime of the analysis was changed: the temperature of the gas sampling valves was reduced to 50 °C, and the heating of the metal capillary through which the sample from the reactor was fed to the gas sampling valves was disabled. The temperature program in the column oven was

50 °C—10 min, temperature rise 5 °C/min to 190 °C. The total analysis time was 60 min or more if necessary. Cyclopropane and propylene peaks were separated to the zero line at the first temperature plateau at 50 °C (see Figure 5).

According to the data from the literature, when using a capillary column with a porous polymer of low polarity (phase type Q), C<sub>3</sub> hydrocarbons are eluted at a sufficient distance from hydrocarbons C<sub>2</sub> and C<sub>4</sub> in the following order: propylene, propane, allene, cyclopropane, methylacetylene (Application A01454 + [71])—see also [68,72]. In this work, five C<sub>3</sub> hydrocarbons were separated and yielded separate peaks in a column oven under the following temperature program: 40 °C—6 min, temperature rise 10 °C/min to 160 °C, total analysis time 40–50 min (see Figures 4b, 6 and S7).

For a capillary column with a polar porous polymer (U-phase), the elution order of the C<sub>3</sub> hydrocarbons was propylene + propane (one peak), cyclopropane, allene, methylacetylene (Applications A01456, CA000C1128 + [73]). In this work, four peaks separated to the zero line were obtained in the C<sub>3</sub> hydrocarbon region when heated in a column oven under the following temperature program: 60 °C—5 min, temperature rise 10 °C/min up to 150 °C (Figures 4c and S8).

### 3.3. Cyclopropane Content in a Mixture of Pyrolysis Products of C<sub>4</sub>–C<sub>5</sub> Alkanes

The results of the analysis of pulse pyrolysis product mixtures of isobutane [19], *n*-butane [20], *n*-pentane [21], and isopentane [22] in an adiabatic compression reactor show that the main products are: hydrogen, methane, ethylene and propylene (see Figures S1 and S2). At temperatures up to  $T_{\max} \approx 1300$  K and correspondingly for alkane conversion degrees  $\leq 80\%$ , the main products of pulsed pyrolysis of C<sub>4</sub>–C<sub>5</sub> isoalkanes also include isobutene, and for *n*-pentane, they include butane-1. Acetylene is added to the main products at a high conversion degree. The list of minor products is quite long, and among them are ethane, propane, allene, methylacetylene, 4 acyclic butenes (butene-1, *trans*- and *cis*-butene-2, isobutene), butadiene-1,3, vinyl acetylene, diacetylene, butene-1, butene-2, six acyclic pentenes (pentene-1, *trans*- and *cis*-pentene-2, 2-methylbuten-1, 2-methylbuten-2, 3-methylbuten-1), cyclopentene, cyclopentadiene, isoprene, benzene, toluene, etc. [19–22]. Along with these substances, previously unidentified products were found in a mixture of products. In particular, in the chromatogram obtained using a CP-Al<sub>2</sub>O<sub>3</sub>/KCl PLOT capillary column, a small peak before the propylene peak was detected (see Figures S3–S6). According to the chemical analysis there are no molecular oxygen and oxygen-containing organic substances in the initial mixtures; moreover, the highly polar substances are not eluted from the alumina columns [74]. Consequently, this small peak can only correspond to hydrocarbons. A comparison of the retention times of the C<sub>2</sub> to C<sub>4</sub> hydrocarbons and this unknown peak shows that it can be matched to the C<sub>3</sub> hydrocarbon but not to the propane, propylene, allene or methylacetylene, whose retention times have been determined. Reference chromatograms of hydrocarbon mixtures on CP-Al<sub>2</sub>O<sub>3</sub>/KCl PLOT capillary columns from the ScanView Application Database [23] show a cyclopropane peak before the propylene peak (see Table 1).

For the final identification of the peak of the unknown C<sub>3</sub> hydrocarbon, a chromatographic analysis of mixtures containing cyclopropane was performed under the same GC analysis conditions as the pyrolysis products of C<sub>4</sub>–C<sub>5</sub> alkanes. Figure 4a shows the chromatograms of the pyrolysis product mixture of *n*-butane (blue line), the mixture 15 ppm *cyclo*-C<sub>3</sub>H<sub>6</sub>/15 ppm C<sub>3</sub>H<sub>6</sub> in Ar (red line) and the reference mixture of 15 ppm C<sub>n</sub>H<sub>m</sub> in N<sub>2</sub> (green line). As can be seen in this figure, the retention times of cyclopropane and the unknown product are the same. In addition, the retention times of the reference mixture and the known pyrolysis products (CH<sub>4</sub>, C<sub>2</sub>H<sub>6</sub>, C<sub>2</sub>H<sub>4</sub>, C<sub>2</sub>H<sub>2</sub>, C<sub>3</sub>H<sub>8</sub>, C<sub>3</sub>H<sub>6</sub>, *n*-C<sub>4</sub>H<sub>10</sub>) present in this chromatogram are identical.

For the C<sub>3</sub> hydrocarbon retention times, chromatograms of pyrolysis product mixtures obtained with the CP-PoraBOND Q and CP-PoraPLOT U, along with propane, propylene, allene and methylacetylene, also show a small peak attributed to cyclopropane according to reference chromatograms from ScanView [23] (see Figure 4b,c). A comparison of the

chromatograms of the product mixtures (blue line), the mixture 15 ppm *cyclo*-C<sub>3</sub>H<sub>6</sub>/15 ppm C<sub>3</sub>H<sub>6</sub> in Ar (red line) and reference mixture 15 ppm C<sub>n</sub>H<sub>m</sub> in N<sub>2</sub> (green line) confirmed the identification of the unknown C<sub>3</sub> hydrocarbon peak as cyclopropane.

In order to rule out the appearance of a small peak before the propylene peak due to thermal degradation processes and misidentification, an additional series of experiments (2a) was carried out on the pyrolysis of *n*-butane (same mixture) at an initial temperature  $T_0 = 323$  K (50 °C). The following were also changed: the temperature regime of injectors and gas sampling valves (the temperature was reduced from 150 °C to 50 °C), the temperature program in the CP-Al<sub>2</sub>O<sub>3</sub>/KCl PLOT column oven (the temperature of the initial section at which the separation of propylene and the small peak in front of it were reduced from 100 °C to 50 °C), and the heating of the metal capillary through which the sample was transferred from the reactor into gas sampling valves was turned off. In all cases, a small peak before the propylene peak was detected when separating the product mixture on the CP-Al<sub>2</sub>O<sub>3</sub>/KCl PLOT column (see Figure 5a) and between the allene and propylene peaks when separating the product mixture on the CP-PoraBOND Q column (see Figure 5b). Thus, it was shown that the presence of a small peak among C<sub>3</sub> hydrocarbons in the chromatograms of the mixture of pyrolysis products of C<sub>4</sub>–C<sub>5</sub> alkanes is not due to temperature effects.

The small C<sub>3</sub> hydrocarbon peak detected on the three PLOT columns cannot be a ghost peak because in the “blank” analysis with argon, there are no peaks in the cyclopropane elution region on any column; the sample fed for analysis is not in contact with the injector (septa, liner, etc.), but is injected from a gas sampling valve directly into the column; the peak identified as cyclopropane is eluted from alumina at an isotherm of 100 °C when analyzed according to the standard program, and at 50 °C when analyzed according to the modified program in an additional series of experiments. There were no acids, bases, alcohols or water in the sample that may have contributed to ghost peaks [75]. There are no peaks caused by previous sample entry—the peak attributed to cyclopropane appeared in the first analysis on all columns.

The dependence of cyclopropane yield on maximum temperature  $T_{\max}$  in a series of experiments with  $T_0 = 393$  K began at temperatures 1150–1160 K, passed through the maximum in the range 1270–1320 K, and decreased monotonously up to the end of the temperature interval for all investigated alkanes, C<sub>4</sub>–C<sub>5</sub> (Figure 6a). The initial sections of cyclopropane yield dependence coincided for all investigated alkanes, but the position of maximums and the final sections were different. The maximum yield of cyclopropane increased with the transition from normal alkanes to isoalkanes and from pentanes to butanes. For isobutene, it reached  $\approx 0.017$  wt. %, and for *n*-pentane, 0.009 wt. %. For all investigated alkanes C<sub>4</sub>–C<sub>5</sub>, the dependences of the ratio of yields of cyclopropane and propylene  $Y_{c-C_3H_6}/Y_{C_3H_6}$  monotonically increased with increasing  $T_{\max}$  (Figure 6b). The maximum value of the  $Y_{c-C_3H_6}/Y_{C_3H_6}$  ratio reached  $7 \times 10^{-4}$  at high temperatures. According to data from the literature, the yields of cyclopropane during the pyrolysis of cyclopentane are markedly higher. For a mixture with an initial cyclopentane concentration of 5%, the ratio  $Y_{c-C_3H_6}/Y_{C_3H_6}$  decreases with increasing temperature from 0.14 to 0.018 [41]. During the decomposition of the cyclopentyl radical, the ratio  $Y_{c-C_3H_6}/Y_{C_3H_6}$  in the products in the temperature range 1060–1116 K ranges from  $3 \times 10^{-3}$  to  $5 \times 10^{-3}$  [47]. During the decomposition of the 1-pentyl radical, the yield of cyclopropane is approximately  $1 \times 10^{-3}$  relative to propylene [46]. The selectivity of cyclopropane for *n*-butane and isobutane, and for *n*-pentane and isopentane, coincides in pairs to a conversion degree of alkane of  $\approx 25\%$  and 30%, respectively (Figure 7). It is seen that in the pyrolysis of C<sub>4</sub>–C<sub>5</sub> acyclic alkanes, cyclopropane is not a primary product, in contrast to the pyrolysis of cyclopentane [41] and the decomposition of cyclopentyl radical [47]. The selectivities of cyclopropane during the pyrolysis of *n*-butane in two series of experiments at different initial temperatures  $T_0 = 393$  K (shaded squares 2) and  $T_0 = 323$  K (shaded rhombus 2a) are similar in shape and differ in the position of the maximum. The results obtained testify not only to the low content of cyclopropane in the products of pulse pyrolysis of acyclic alkanes C<sub>4</sub>–C<sub>5</sub>,

but also to the difference in the mechanism of its formation compared to the pyrolysis of cyclopentane.

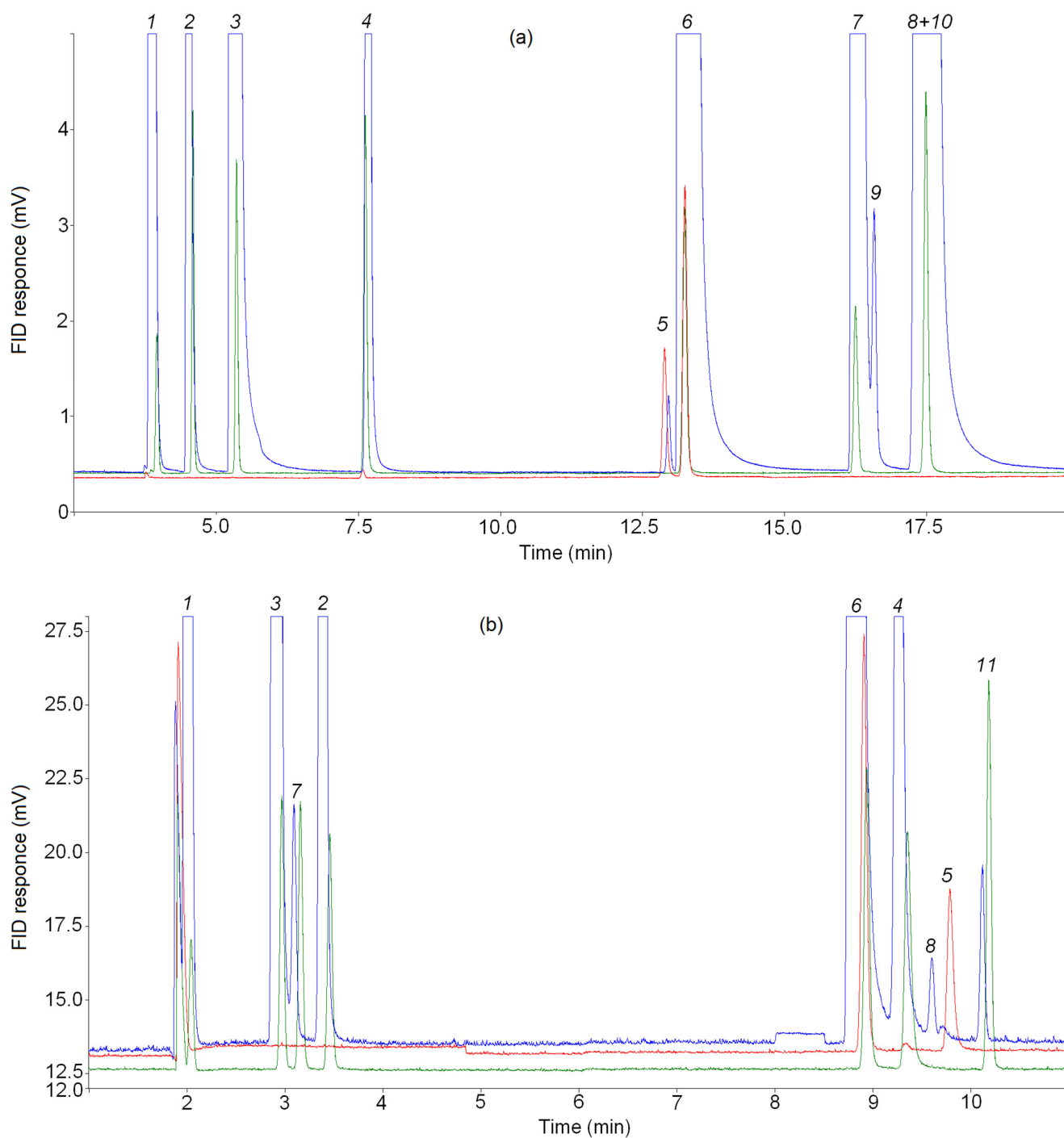


**Figure 5.** Representative chromatogram from (a) the CP- $\text{Al}_2\text{O}_3/\text{KCl}$  PLOT and (b) the CP-PoraBOND Q columns, zoomed view. The analysis conditions have changed (see text). Blue line—products of *n*-butane pyrolysis (additional series at  $T_0 = 323$  K), red line—reference mixture *cyclo*- $\text{C}_3\text{H}_6/15$  ppm  $\text{C}_3\text{H}_6$  in Ar, green line—reference mixture 15 ppm  $\text{C}_n\text{H}_m$  in  $\text{N}_2$ . Note that the larger peaks are off-scale to allow observation of the minor products. Identified compounds: 1 = methane; 2 = ethane; 3 = ethylene; 4 = propane; 5 = cyclopropane; 6 = propylene; 7 = acetylene; 8 = allene; 9 = isobutane; 10 = *n*-butane, 11 = methylacetylene.

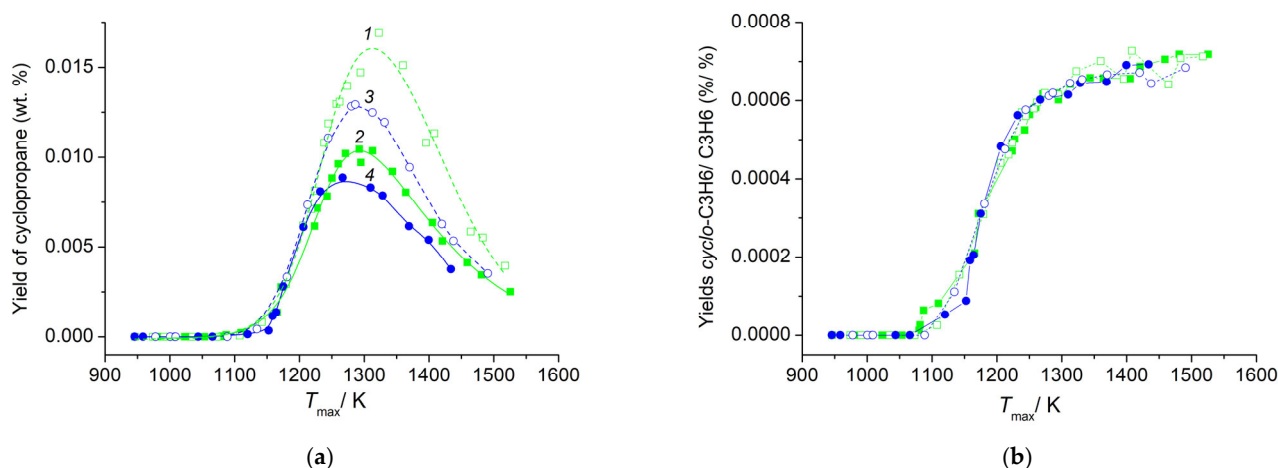


**Figure 6.** Temperature dependence of the cyclopropane yield (a) and  $Y_{C-C_3H_6}/Y_{C_3H_6}$  (b). Open squares (1), closed squares (2), open circle (3) and closed circles (4) represent the weight content of cyclopropane produced during the pyrolysis of isobutane, *n*-butane, isopentane and *n*-pentane, respectively. Initial temperature  $T_0 = 393$  K.

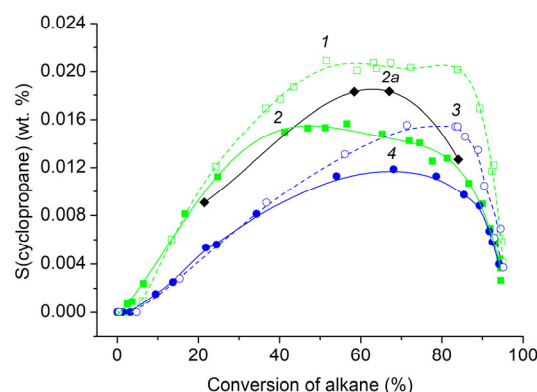


**Figure 7.** Selectivity of the cyclopropane. Symbols (1)–(4) are the same as in Figure 6. The closed rhombus (2a) represents the selectivity of the cyclopropane produced during the pyrolysis of *n*-butane at the initial temperature  $T_0 = 323$  K.

Thus, among the products of the pyrolysis of *n*-butane, isobutane, *n*-pentane and isopentane, cyclopropane was found for the first time in small quantities. Surprisingly, a stressed cyclic hydrocarbon is formed in the non-selective gas-phase pyrolysis process of alkanes. The presence of cyclopropane in the pyrolysis products of alkanes means that the rate of its formation is comparable to the rate of decline. It is known that at high temperatures, cyclopropane is rapidly isomerized into propylene, so the rate of the formation of cyclopropane should also be high enough. Detailed kinetic mechanisms involving cyclopropane are discussed in the literature [76–78], but all of them were developed for modeling ignition delays, and are not adapted for the study of the kinetics of cyclopropane formation in an oxygen-free environment. The question about the mechanism of cyclopropane formation under the conditions of pulse pyrolysis of alkanes remains open. Further theoretical and experimental investigations are desirable to establish the mechanism of this reaction.

#### 4. Conclusions

The pulsed pyrolysis of  $C_4$ – $C_5$  alkanes with normal and isomeric structures was studied in an adiabatic compression reactor with a free flying piston. The composition of the pulsed pyrolysis products was investigated by gas chromatography. The analysis of the hydrocarbon part of the products was carried out using three capillary columns of different polarity and selectivity, and sufficient efficiency to separate all  $C_1$ – $C_4$  hydrocarbons (CP-

Al<sub>2</sub>O<sub>3</sub>/KCl PLOT column) and C<sub>1</sub>–C<sub>3</sub> hydrocarbons (CP-PoraBOND Q and CP-PoraPLOT columns). Cyclopropane was found among the pyrolysis products for the first time. The identification of cyclopropane in the products of pulsed pyrolysis of C<sub>4</sub>–C<sub>5</sub> alkanes was carried out by analyzing mixtures containing cyclopropane and other C<sub>1</sub>–C<sub>4</sub> hydrocarbons under the same conditions as the standard analysis of a mixture of products. The peak attributed to cyclopropane cannot be a ghost peak. This was confirmed in a series of experiments on the pyrolysis of *n*-butane with a reduced initial temperature of the adiabatic compression reactor (from 120 °C to 50 °C) and a modified GC analysis mode.

Cyclopropane yields, as a function of maximum temperature, show a bell-shaped, asymmetrical dependence. The maximum yield of cyclopropane increases with the transition from normal alkanes to isoalkanes and from pentanes to butanes. For isobutene, it reaches ≈0.017 wt. %, and for *n*-pentane, 0.009 wt. %. Cyclopropane is not a primary product of the pyrolysis of isobutane, *n*-butane, isopentane or *n*-pentane, unlike cyclopentane.

Thus, the conducted studies indicate the formation of cyclopropane during the pyrolysis of C<sub>4</sub>–C<sub>5</sub> alkanes with normal and isomeric structures. Further theoretical and experimental studies are desirable to establish the mechanism of this reaction. It should be noted that substances such as cyclopropane can be detected in a mixture of products during rapid cooling (quenching), which was successfully implemented in the method of the adiabatic compression of gases with a free flying piston.

**Supplementary Materials:** The following supporting information can be downloaded at: <https://www.mdpi.com/article/10.3390/reactions4030023/s1>, Figure S1: Representative chromatograms of *n*-butane pyrolysis products and the initial mixture from the CP-Al<sub>2</sub>O<sub>3</sub>/KCl PLOT column under standard analysis conditions; Figure S2: Representative chromatograms of isobutane pyrolysis products and the initial mixture from the CP-Al<sub>2</sub>O<sub>3</sub>/KCl PLOT column under standard analysis conditions; Figure S3: Representative chromatograms of *n*-butane pyrolysis products and the initial mixture from the CP-Al<sub>2</sub>O<sub>3</sub>/KCl PLOT column under standard analysis conditions—zoomed view; Figure S4: Representative chromatograms of isobutane pyrolysis products and the initial mixture from the CP-Al<sub>2</sub>O<sub>3</sub>/KCl PLOT column under standard analysis conditions—zoomed view; Figure S5: Representative chromatograms of *n*-pentane pyrolysis products and the initial mixture from the CP-Al<sub>2</sub>O<sub>3</sub>/KCl PLOT column under standard analysis conditions—zoomed view; Figure S6: Representative chromatograms of isopentane pyrolysis products and the initial mixture from the CP-Al<sub>2</sub>O<sub>3</sub>/KCl PLOT column under standard analysis conditions—zoomed view; Figure S7: Representative chromatograms of isobutane pyrolysis products and the initial mixture from the CP-PoraBOND Q column under standard analysis conditions—zoomed view; Figure S8: Representative chromatograms of isobutane pyrolysis products and the initial mixture from the CP-PoraPLOT U column—zoomed view.

**Funding:** This work was carried out within the State Program for the TIPS RAS.

**Data Availability Statement:** The data presented in this study are available on request from the corresponding author. The data are not publicly available due to restrictions privacy.

**Conflicts of Interest:** The authors declare no conflict of interest.

## References

1. Longwell, P.A.; Reamer, H.H.; Wilburn, N.P.; Sage, B.H. Ballistic piston for investigating gas phase reactions. *Ind. Eng. Chem.* **1958**, *50*, 603–610. [[CrossRef](#)]
2. Markevich, A.M.; Azatyan, V.V.; Sokolova, N.A. Adiabatic compression as a method for studying chemical processes under nonstationary conditions. *Kinet. Catal.* **1962**, *3*, 431–438.
3. Volokhonovich, I.E.; Markevich, A.M.; Masterovoy, I.F.; Azatyan, V.V. Non-isothermal processes. Thermal cracking of methane. *Dokl. USSR* **1962**, *146*, 387–390.
4. Kondratiev, V.N. Determination of the rate constant for thermal cracking of methane by means of adiabatic compression and expansion. *Symp. Int. Combust.* **1965**, *10*, 319–322. [[CrossRef](#)]
5. Buravtsev, N.N.; Grigor'ev, A.S.; Kolbanovskii, Y.A. Kinetics of the cyclodimerization of tetrafluoroethylene and the thermal decomposition of octafluorocyclobutane. *Kinet. Catal.* **1985**, *26*, 1–7.

6. Buravtsev, N.N.; Grigor'ev, A.S.; Kolbanovskii, Y.A. Kinetics and mechanism of pyrolysis of hexafluoropropylene. *Kinet. Catal.* **1989**, *30*, 13–22.
7. Kuptsova, T.S.; Buravtsev, N.N.; Chernyak, N.Y.; Shapiro, E.A.; Kolbanovskii, Y.u.A.; Nefedov, O.M. Thermal isomerization of 3,3-dimethylcyclopropene under adiabatic-compression conditions. *Russ. Chem. Bull.* **1989**, *38*, 1845–1847. [[CrossRef](#)]
8. Kolbanovskiy, Y.A. Adiabatic compression in studies on the kinetics and mechanism of reactions involving fluorine-containing carbenes. *Russ. Chem. Rev.* **1989**, *58*, 1024–1032. [[CrossRef](#)]
9. Ryabinin, Y.N. *Gases at High Densities and Temperatures*; Pergamon Press, Inc.: New York, NY, USA, 1961; 52p.
10. Lalos, G.T.; Hammond, G.L. The Ballistic Compression and High Temperature Properties of Dense Gases. In *Experimental Thermodynamics, Volume II. Experimental Thermodynamics of Non-Reacting Fluids*; Le Neindre, B., Vodar, B., Eds.; Springer Science + Business Media: New York, NY, USA, 1975; pp. 1193–1218.
11. Kolbanovskiy, Y.A.; Shchipachev, V.S.; Chernyak, N.Y.; Chernyshova, A.S.; Grigor'ev, A.S. *Impulsive Compression of Gases in Chemistry and Technology*; Science: Moscow, Russia, 1982; 240p. (In Russian)
12. Buravtsev, N.N.; German, L.S.; Grigor'ev, A.S.; Kolbanovskii, Y.A.; Ovsiannikov, A.A.; Volkonskii, A.Y. Trifluoromethylfluorocarbene Formation and Reactions under C<sub>2</sub>F<sub>5</sub>SiF<sub>3</sub> Pulsed Adiabatic Compression Pyrolysis. *Mendeleev Commun.* **1993**, *3*, 133–134. [[CrossRef](#)]
13. Slotboom, Y.; Roosjen, S.; Kronberg, A.; Glushenkov, M.; Kersten, S.R.A. Methane to ethylene by pulsed compression. *Chem. Eng. J.* **2021**, *414*, 128821. [[CrossRef](#)]
14. Drost, S.; Schießl, R.; Maas, U. Multi compression–expansion process for chemical energy conversion: Transformation of methane to unsaturated hydrocarbons and hydrogen. *Appl. Energy Combust. Sci.* **2023**, *14*, 100129. [[CrossRef](#)]
15. Porras, S.; Kaczmarek, D.; Herzler, J.; Drost, S.; Werler, M.; Kasper, T.; Fikri, M.; Schießl, R.; Atakan, B.; Schulz, C.; et al. An experimental and modeling study on the reactivity of extremely fuel-rich methane/dimethyl ether mixtures. *Combust. Flame* **2020**, *212*, 107–122. [[CrossRef](#)]
16. Ezdin, B.S.; Vasiljev, S.A.; Yatsenko, D.A.; Fedorov, V.E.; Ivanova, M.N.; Kalyada, V.V.; Pakharukov, Y.V.; Shabiev, F.K.; Zarvin, A.E. The Synthesis of Carbon Nanoparticles in a Compression Reactor in the Atmosphere of Buffer Gases. *Sib. J. Phys.* **2022**, *17*, 29–46. [[CrossRef](#)]
17. Rudolph, C.; Atakan, B. Pyrolysis of Methane and Ethane in a Compression–Expansion Process as a New Concept for Chemical Energy Storage: A Kinetic and Exergetic Investigation. *Energy Technol.* **2021**, *9*, 2000948. [[CrossRef](#)]
18. Ashok, A.; Katebah, M.A.; Linke, P.; Kumar, D.; Arora, D.; Fischer, K.; Jacobs, T.; Al-Rawashdeh, M. Review of piston reactors for the production of chemicals. *Rev. Chem. Eng.* **2023**, *39*, 1–30. [[CrossRef](#)]
19. Bilera, I.V.; Buravtsev, N.N. The homogeneous pyrolysis of isobutane under pulsed adiabatic compression. *Gorenie Vzryv. Mosk.—Combust. Explos.* **2013**, *6*, 37–40.
20. Bilera, I.V. The homogeneous pyrolysis of *n*-butane under pulsed adiabatic compression. *Gorenie Vzryv. Mosk.—Combust. Explos.* **2014**, *7*, 35–41.
21. Bilera, I.V. The homogeneous pyrolysis of *n*-pentane under pulsed adiabatic compression. *Gorenie Vzryv. Mosk.—Combust. Explos.* **2015**, *8*, 97–105.
22. Bilera, I.V.; Buravtsev, N.N. The homogeneous pyrolysis of isopentane under pulsed adiabatic compression. *Gorenie Vzryv. Mosk.—Combust. Explos.* **2016**, *9*, 74–82.
23. ScanView—Online eLibrary (Agilent Technologies). The Fully Updated 2018 Version Is Available and Is Hosted in Agilent Community. Available online: <https://community.agilent.com> (accessed on 16 October 2018).
24. Allara, D.L.; Edelson, D. A Computational Modeling Study of the Low-Temperature Pyrolysis of *n*-Alkanes; Mechanisms of Propane, *n*-Butane, and *n*-Pentane Pyrolyses. *Int. J. Chem. Kinet.* **1975**, *7*, 479–507. [[CrossRef](#)]
25. Safarik, I.; Strausz, O.P. The thermal decomposition of hydrocarbons. Part 1. *n*-alkanes (C ≥ 5). *Res. Chem. Intermed.* **1996**, *22*, 275–314. [[CrossRef](#)]
26. Dente, M.; Bozzano, G.; Faravelli, T.; Marongiu, A.; Pierucci, S.; Ranzi, E. Kinetic Modelling of Pyrolysis Processes in Gas and Condensed Phase. *Adv. Chem. Eng.* **2007**, *32*, 51–166. [[CrossRef](#)]
27. Hou, X.; Song, C.; Ma, Z.; Chen, B.; Zhao, L.; Huang, J.; Yuan, E.; Cui, T. Universality analysis of the reaction pathway and product distribution in C<sub>5</sub>–C<sub>10</sub> *n*-alkanes pyrolysis. *J. Anal. Appl. Pyrolysis* **2022**, *162*, 105451. [[CrossRef](#)]
28. Zamostny, P.; Belohlav, Z.; Starkbaumova, L.; Patera, J. Experimental study of hydrocarbon structure effects on the composition of its pyrolysis products. *J. Anal. Appl. Pyrolysis* **2010**, *87*, 207–216. [[CrossRef](#)]
29. Yanovskaya, L.A.; Dombrovskii, V.A. Functionally Substituted Cyclopropanes. *Russ. Chem. Rev.* **1975**, *44*, 154–169. [[CrossRef](#)]
30. Lebel, H.; Marcoux, J.-F.; Molinaro, C.; Charette, A.B. Stereoselective Cyclopropanation Reactions. *Chem. Rev.* **2003**, *103*, 977–1050. [[CrossRef](#)]
31. Vogel, E. Kleine Kohlenstoff-Ringe. *Angew. Chem.* **1960**, *72*, 4–26. [[CrossRef](#)]
32. Engel, P.S. Mechanism of the thermal and photochemical decomposition of azoalkanes. *Chem. Rev.* **1980**, *80*, 99–150. [[CrossRef](#)]
33. Elinson, M.N.; Dorofeeva, E.O.; Vereshchagin, A.N.; Nikishin, G.I. Electrochemical synthesis of cyclopropanes. *Russ. Chem. Rev.* **2015**, *84*, 485–497. [[CrossRef](#)]
34. Ebner, C.; Carreira, E.M. Cyclopropanation Strategies in Recent Total Syntheses. *Chem. Rev.* **2017**, *117*, 11651–11679. [[CrossRef](#)]
35. Lott, W.A.; Christiansen, W.G. The preparation of cyclopropane. *J. Am. Pharm. Assoc.* **1930**, *19*, 341–344. [[CrossRef](#)]

36. Setser, D.W.; Rabinovitch, B.S. Singlet methylene from thermal decomposition of diazomethane. Unimolecular reactions of chemically activated cyclopropane and dimethylcyclopropane molecules. *Can. J. Chem.* **1962**, *40*, 1425–1451. [CrossRef]
37. Setser, D.W.; Rabinovitch, B.S.; Simons, J.W. Collisional Transition Probabilities for Deactivation of Highly Vibrationally Excited Cyclopropane and Dimethylcyclopropane. *J. Chem. Phys.* **1964**, *40*, 1751–1761. [CrossRef]
38. Crawford, R.J.; Mishra, A. The Mechanism of the Thermal Decomposition of 1-Pyrazolines and Its Relationship to Cyclopropane Isomerizations. *J. Am. Chem. Soc.* **1966**, *88*, 3963–3969. [CrossRef]
39. Campbell, R.J.; Schlag, E.W.; Ristow, B.W. Mechanistic consequences of curved Stern–Volmer plots. The photolysis of cyclobutanone. *J. Am. Chem. Soc.* **1967**, *89*, 5098–5102. [CrossRef]
40. Blades, A.T. Kinetics of the thermal decomposition of cyclobutanone. *Can. J. Chem.* **1969**, *47*, 615–617. [CrossRef]
41. Tsang, W. Thermal decomposition of cyclopentane and related compounds. *Int. J. Chem. Kinet.* **1978**, *10*, 599–617. [CrossRef]
42. Gusel'nikov, L.E.; Volkova, V.V.; Ivanov, P.E.; Inyushkin, S.V.; Shevelkova, L.V.; Zimmermann, G.; Ziegler, U.; Ondruschka, B. Direct infrared spectroscopic evidence of allyl radical and definition of the initiation step in thermal decomposition of cycloalkanes. A comparison with very low pressure pyrolysis of alkenes. *J. Anal. Appl. Pyrolysis* **1991**, *21*, 79–93. [CrossRef]
43. Tsang, W. Thermal stability of cyclohexane and 1-hexene. *Int. J. Chem. Kinet.* **1978**, *10*, 1119–1138. [CrossRef]
44. Wang, Z.; Cheng, Z.; Yuan, W.; Cai, J.; Zhang, L.; Zhang, F.; Qi, F.; Wang, J. An experimental and kinetic modeling study of cyclohexane pyrolysis at low pressure. *Combust. Flame* **2012**, *159*, 2243–2253. [CrossRef]
45. Awan, I.A.; McGivern, W.S.; Tsang, W.; Manion, J.A. Decomposition and isomerization of 5-methylhex-1-yl radical. *J. Phys. Chem. A* **2010**, *114*, 7832–7846. [CrossRef]
46. Awan, I.A.; Burgess, D.R., Jr.; Manion, J.A. Pressure Dependence and Branching Ratios in the Decomposition of 1-Pentyl Radicals: Shock Tube Experiments and Master Equation Modeling. *J. Phys. Chem. A* **2012**, *116*, 2895–2910. [CrossRef]
47. Awan, I.A.; Burgess, D.R., Jr.; Tsang, W.; Manion, J.A. Shock tube study of the decomposition of cyclopentyl radicals. *Proc. Combust. Inst.* **2011**, *33*, 341–349. [CrossRef]
48. Manion, J.A.; Awan, I.A. A Shock tube study of H atom addition to cyclopentene. *Int. J. Chem. Kinet.* **2018**, *50*, 225–242. [CrossRef]
49. Markus, M.W.; Woiki, D.; Roth, P. Two-channel thermal decomposition of CH<sub>3</sub>. *Proc. Combust. Inst.* **1992**, *24*, 581–588. [CrossRef]
50. Saldana, M.H.; Bogin, G.E., Jr. Investigation of *n*-pentane pyrolysis at elevated temperatures and pressures in a variable pressure flow reactor. *J. Anal. Appl. Pyrolysis* **2016**, *118*, 286–297. [CrossRef]
51. Zhang, Y.-J.; Yuan, W.-H.; Cai, J.-H.; Zhang, L.-D.; Qi, F.; Li, Y.-Y. Product identification and mass spectrometric analysis of *n*-butane and *i*-butane pyrolysis at low pressure. *Chin. J. Chem. Phys.* **2013**, *26*, 151–156. [CrossRef]
52. Li, W.; Wang, G.; Li, Y.; Li, T.; Zhang, Y.; Cao, C.; Zou, J.; Law, C.K. Experimental and kinetic modeling investigation on pyrolysis and combustion of *n*-butane and *i*-butane at various pressures. *Combust. Flame* **2018**, *191*, 126–141. [CrossRef]
53. Goos, E.; Hippler, H.; Hoyermann, K.; Jürges, B. Laser powered homogeneous pyrolysis of butane initiated by methyl radicals in a quasi-wall-free reactor at 750–1000 K. *Phys. Chem. Chem. Phys.* **2000**, *2*, 5127–5132. [CrossRef]
54. Khan, Z.A.; Hellier, P.; Ladommatos, N.; Almaleki, A. Sampling of Gas-Phase Intermediate Pyrolytic Species at Various Temperatures and Residence Times during Pyrolysis of Methane, Ethane, and Butane in a High-Temperature Flow Reactor. *Sustainability* **2023**, *15*, 6183. [CrossRef]
55. Sirjean, B.; Glaude, P.A.; Ruiz-Lopez, M.F.; Fournet, R. Detailed kinetic study of the ring opening of cycloalkanes by CBS-QB3 calculations. *J. Phys. Chem. A* **2006**, *110*, 12693–12704. [CrossRef] [PubMed]
56. Alkidas, A.C.; Plett, E.G.; Summerfield, M. Performance study of a ballistic compressor. *AIAA J.* **1976**, *14*, 1752–1758. [CrossRef]
57. Price, D.; Lalos, G.T. Adiabatic compressor for *P-V-T* measurements on gases to 100,000 pounds per square inch. *Ind. Eng. Chem.* **1957**, *49*, 1987–1992. [CrossRef]
58. Castello, G.; Vezzani, S.; Gardella, L. Influence of temperature on the polarity of porous polymer beads stationary phases for gas chromatography. *J. Chromatogr. A* **1999**, *837*, 153–170. [CrossRef]
59. Ji, Z.; Majors, R.E.; Guthrie, E.J. Porous layer open-tubular capillary columns: Preparations, applications and future directions. *J. Chromatogr. A* **1999**, *842*, 115–142. [CrossRef]
60. Grob, R.L.; Kaiser, M.A. Qualitative and Quantitative Analysis by Gas Chromatography. In *Modern Practice of Gas Chromatography*, 4th ed.; Grob, R.L., Barry, E.F., Eds.; John Wiley & Sons, Inc.: Hoboken, NJ, USA, 2004; pp. 403–460.
61. Do, L.; Raulin, F. Gas chromatography of Titan's atmosphere. III. Analysis of low-molecular-weight hydrocarbons and nitriles with a CP-Sil5 CB WCOT capillary column. *J. Chromatogr.* **1992**, *591*, 297–301. [CrossRef]
62. Armstrong, D.W.; Reid, G.L.; Luong, J. Gas Separations: A Comparison of GasPro™ and Aluminum Oxide PLOT Columns for the Separation of Highly Volatile Compounds. *Curr. Sep.* **1996**, *15*, 5–11. Available online: <http://www.currentseparations.com/issues/15-1/cs15-1a.pdf> (accessed on 16 March 2023).
63. Ji, Z.; Chang, I. A New Look at Light Hydrocarbon Separations on Commercial Alumina PLOT Columns: Column Selectivity and Separation. *J. High Resolut. Chromatogr.* **1996**, *19*, 32–36. [CrossRef]
64. Schneider, W.; Frone, J.; Bruderreck, H. Determination of hydrocarbons in the parts per 10<sup>9</sup> range using glass capillary columns coated with aluminium oxide. *J. Chromatogr.* **1978**, *155*, 311–327. [CrossRef]
65. De Nijs, R.C.M. Analysis of Light Hydrocarbons C<sub>1</sub>–C<sub>5</sub> with Porous Layer Open Tubular Fused Silica Columns of Aluminum Oxide. *J. High Resolut. Chromatogr.* **1981**, *4*, 612–615. [CrossRef]
66. De Nijs, R.C.M.; De Zeeuw, J. Aluminium oxide-coated fused-silica porous-layer open-tubular column for gas-solid chromatography of C<sub>1</sub>–C<sub>10</sub> hydrocarbons. *J. Chromatogr.* **1983**, *279*, 41–48. [CrossRef]

67. De Zeeuw, J.; De Nijs, R.C.M.; Henrich, L.T. Adsorption Chromatography on PLOT (Porous-Layer Open-Tubular) Columns: A New Look at the Future of Capillary GC. *J. Chromatogr. Sci.* **1987**, *25*, 71–83. [[CrossRef](#)]
68. Henrich, L.H. Recent Advances in Adsorption Chromatography for Analysis of Light Hydrocarbons in Petrochemical-Related Materials. *J. Chromatogr. Sci.* **1988**, *26*, 198–205. [[CrossRef](#)]
69. Schaeffer, H.-J. Gas Chromatographic Analysis of Traces of Light Hydrocarbons. A Review of Different Systems in Practice. *J. High Resolut. Chromatogr.* **1989**, *12*, 69–81. [[CrossRef](#)]
70. De Zeeuw, J.; Luong, J. Developments in stationary phase technology for gas chromatography. *Trends Anal. Chem.* **2002**, *21*, 594–607. [[CrossRef](#)]
71. Tang, Y.-Z.; Tran, Q.; Fellin, P.; Cheng, W.K.; Drummond, I. Determination of C<sub>1</sub>–C<sub>4</sub> hydrocarbons in air. *Anal. Chem.* **1993**, *65*, 1932–1935. [[CrossRef](#)]
72. Do, L.; Raulin, F. Gas chromatography of Titan's atmosphere. I. Analysis of low-molecular-weight hydrocarbons and nitriles with a PoraPLOT Q porous polymer coated open-tubular capillary column. *J. Chromatogr.* **1989**, *481*, 45–54. [[CrossRef](#)]
73. Ji, Z.; Hutt, S. A New Bonded Porous Polymer PLOT U Column with Increased Polarity. *J. Chromatogr. Sci.* **2000**, *38*, 496–502. [[CrossRef](#)]
74. Ruan, Z.; Liu, H.J. Preparation of 4-vinylpyridine and divinylbenzene porous-layer open tubular columns by in situ copolymerization. *J. Chromatogr.* **1995**, *693*, 79–88. [[CrossRef](#)]
75. Kumar, A.; Sharma, C. Recent update of the various sources originating ghost peaks in gas chromatography: A review. *J. Chromatogr. A* **2022**, *1685*, 463625. [[CrossRef](#)]
76. Battin-Leclerc, F. Detailed chemical kinetic models for the low-temperature combustion of hydrocarbons with application to gasoline and diesel fuel surrogates. *Progr. Energy Combust. Sci.* **2008**, *34*, 440–498. [[CrossRef](#)]
77. Vlasov, P.A.; Garmash, A.A.; Tereza, A.M. Ignition of Cyclopropane in Shock Waves. *Russ. J. Phys. Chem. B* **2016**, *10*, 602–614. [[CrossRef](#)]
78. Wang, R.; Xu, P.; Tang, W.; Ding, T.; Zhang, C.; Li, X. An experimental and kinetic study of the ignition delay characteristics of cyclopropane in air. *Fuel* **2022**, *319*, 123784. [[CrossRef](#)]

**Disclaimer/Publisher's Note:** The statements, opinions and data contained in all publications are solely those of the individual author(s) and contributor(s) and not of MDPI and/or the editor(s). MDPI and/or the editor(s) disclaim responsibility for any injury to people or property resulting from any ideas, methods, instructions or products referred to in the content.